Dynamic Studies on Kinetic H_2/D_2 Quantum Sieving in a Narrow Pore Metal–Organic Framework Grown on a Sensor Chip

Benjamin Paschke,[a] Dmytro Denysenko†,[b] Björn Bredenkötter,[b] German Sastre,*[c]
Achim Wixforth,*[a] and Dirk Volkmer*[b]

Abstract: The separation of deuterium from hydrogen still remains a challenging and industrially relevant task. Compared to traditional cryogenic methods for separation, based on different boiling points of H_2 and D_2, the use of ultramicroporous materials offers a more efficient alternative method. Due to their rigid structures, permanently high porosity, tunable pore sizes and adjustable internal surface properties, metal–organic frameworks (MOFs), a class of porous materials built through the coordination between organic linkers and metal ions/clusters, are more suitable for this approach than zeolites or carbon-based materials. Herein, dynamic gas flow studies on H_2/D_2 quantum sieving in MFU-4, a metal-organic framework with ultra-narrow pores of 2.5 Å, are presented. A specially designed sensor with a very fast response based on surface acoustic waves is used. On-chip measurements of diffusion rates in the temperature range 27–207 K reveal a quantum sieving effect, with D_2 diffusing faster than H_2 below 64 K and the opposite selectivity above this temperature. The experimental results obtained are confirmed by molecular dynamic simulation regarding quantum sieving of H_2 and D_2 on MOFs for which a flexible framework approach was used for the first time.

Deuterium is essential for industrial and academic applications, such as heavy water moderated fission reactors, neutron scattering, NMR spectroscopy, and tracing in metabolic pathways. Due to its high technical demand, the separation of deuterium from hydrogen still remains a challenging and industrially relevant task. Cryogenic methods for separation based on different boiling points of H_2 (20.3 K) and D_2 (23.6 K) give a selectivity of 3 at 20 K.[1] The use of microporous materials offers a more efficient alternative method based on the quantum sieving (QS) effect. This term, first introduced in 1995, describes a phenomenon appearing at low temperatures when the difference between the pore size and molecular diameter of the adsorbate becomes comparable to the de Broglie wavelength of the adsorbate.[2] In this case, the heavier isotope will have a lower zero-point energy, resulting in its faster diffusion compared to the lighter isotope. The different de Broglie wavelengths of H_2 and D_2 at 77 K ($\approx$1.8 and 1.2 Å, respectively),[3] indicate a smaller molecular diameter for D_2 with respect to H_2. With the molecular diameters of H_2/D_2 estimated in the range of 2.4–3.1 Å, we can expect that QS might occur in ultramicropores with aperture widths of <5 Å, approximately. Such small pores can be found in zeolites, carbon-based materials, and metal-organic frameworks (MOFs). Although many theoretical and computational investigations on QS have been performed,[4–6] only a limited number of microporous materials have been tested for QS separation of H_2/D_2,[1] such as zeolites,[7] porous carbons,[3,8] MOFs,[9–11] and covalent–organic frameworks (COFs).[11,12]

In most cases the H_2/D_2 selectivity has been determined from the amounts taken up under certain (non)equilibrium conditions (i.e. from H_2 and D_2 adsorption isotherms or from desorption measurements on samples loaded with H_2/D_2 mixtures). However, it is difficult to optimize the separation conditions using this approach because the obtained selectivity is influenced by many different factors (such as temperature, pressure, loading time, etc.). Since QS relies on different diffusion rates of isotopologues, direct kinetic measurements are highly preferable for studying and optimizing QS-based separation processes. Up until now, only very few dynamic studies on H_2/D_2 QS have been performed. Kinetic profiles of H_2 and D_2 uptake in microporous carbons[3] and $Zn_3(bdc)_3[Cu(pyen)]$ MOF[9] were obtained by monitoring time-dependent weight change in a closed system. However, the diffusion kinetics in such measurements might be influenced by the pressure change with time and, therefore, studies under constant pressure or gas flow are preferable. So far, gas flow studies on H_2/D_2 QS have only once been reported for zeolites and carbon-based materials employing an external mass spectrometer as a detector.[13]

Herein, we report on dynamic gas flow studies on H_2/D_2 QS in MFU-4 metal–organic framework ($[Zn_5Cl_4(BBTA)_3]$, H_2-BBTA =

---

[a] Dr. B. Paschke, Prof. Dr. A. Wixforth
Chair for Experimental Physics I, Institute of Physics
University of Augsburg, Universitätsstrasse 1, 86159 Augsburg (Germany)
E-mail: achim.wixforth@physik.uni-augsburg.de

[b] Dr. D. Denysenko, Dr. B. Bredenkötter, Prof. Dr. D. Volkmer
Chair for Solid State and Materials Chemistry, Institute of Physics
University of Augsburg, Universitätsstrasse 1, 86159 Augsburg (Germany)
E-mail: dirk.volkmer@physik.uni-augsburg.de

[c] Dr. G. Sastre
Instituto de Tecnologia Quimica, Universitat Politecnica de Valencia-Consejo Superior, de Investigaciones Cientificas, Avenida de los Naranjos s/n, 46022 Valencia (Spain)
E-mail: gsastre@itq.upv.es

[†] Deceased 1st June, 2018.

1*H*,5*H*-benzo(1,2-*d*:4,5-*d*′)bistriazole)[14] using a specially designed sensor with a very fast response and based on surface acoustic waves (SAWs).[15a] The technical design of our MOF@SAW device architecture has been described in a previous publication,[16] in which thin films of metal-organic frameworks (MOFs) with different pore sizes were grown on a surface acoustic wave (SAW) substrate, resulting in very sensitive and specific sensor systems for the detection of various gases (CO_2, H_2, He, NH_3, and H_2O) at very short time scales. We were able to show that such a MOF@SAW sensor responds within milliseconds to gas loading and its sensitivity reaches levels as low as 1 ppmv. This unique combination of sensitivity and fast response characteristics allows even for real-time investigations of the sorption kinetics during gas uptake and release. In order to push the technical limits even further we herein report on the temperature-dependent response characteristics of this sensor design on the quantitative differences in the intracrystalline gas diffusion of two isotopologues, namely H_2 and D_2, for which case, to the best of our knowledge, no real-time measurements have been reported before.

SAW sensors are widely used devices that can incorporate MOF thin films for fast, ultrasensitive, inexpensive, and selective detection of gases, with applications such as environmental monitoring, chemical threat detection, food quality control, and medical diagnosis.[15b–e,16,17] Implementation of MOFs in electronic and sensing devices is a highly interesting and promising research field.[18]

In our experiments, MFU-4 was grown directly from the solution on the active sensor area forming a monolayer of single crystals, as described recently.[16] The applied SAW sensor consists of three IDTs, consisting of two comblike interdigitated metal electrodes, defining the wavelength of the SAW on the chip,[19] a piezoelectric substrate ($LiNbO_3$). One centre IDT is employed to generate the SAWs by applying a high frequency signal to it and two outer IDTs to detect both SAWs making use of the reverse effect of the generation. The delay lines of SAWs between each outer and the centre IDT are used as sensitive areas to detect molecular weights in terms of the relative phase shift of both SAWs in a homodyne mixed signal. The functional principle of such sensors is based on porous materials capturing gas molecules on the surface of a SAW propagation path. In particular, to detect mass differences in MOFs by gas adsorption, one delay line is covered with MOF single crystals and the other uncovered delay line is used as a reference channel. This MOF@SAW sensor responds within milliseconds to gas loadings as low as 1 ppmv and allows for real-time monitoring of gas uptake, as has recently been demonstrated for small gas molecules such as CO_2 and N_2.[16]

For measurements at very low temperatures, a specially designed reactor chamber is required (cf. Figure S1, Supporting Information). In this chamber, both the sensor and the supplying gas are cooled down to the respective test temperature in order to ensure complete thermalization and constant temperature for precise measurement of diffusion kinetics. Neon is used as an inert carrier gas because its boiling point of 27.1 K is close to those of the hydrogen isotopologues. Furthermore, Ne atoms cannot enter the framework of MFU-4 owing to their kinetic diameter and thus do not affect the adsorption of H_2 and D_2 (Section S3, Supporting Information).

The characterization of MFU-4 for quantum sieving was performed by detecting the adsorption rates of test gas pulses in a carrier gas flow in real time at various temperatures. The gas pulse measurements show that the phase shifts and, consequently, the mass loading increases with decreasing temperature due to larger physisorption at lower temperature, while the adsorption rate decreases (cf. Figure S2, Supporting Information). Temperature dependence of the diffusion rate constants (k) for H_2 and D_2, determined from time-dependent uptake profiles (cf. Figure S2, Supporting Information), shows the crossover temperature T_c of 64 K (Figure 1 a).

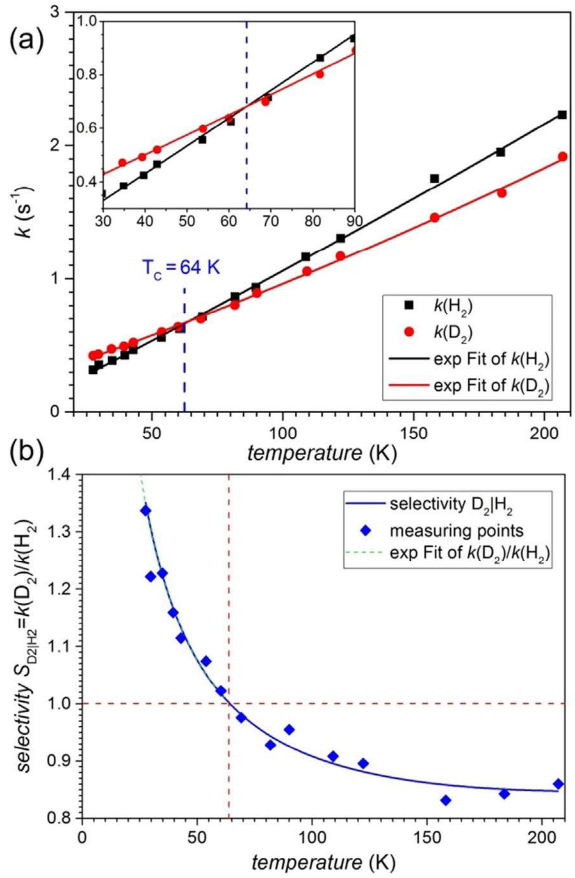

Figure 1. a) Temperature dependence of the rate constants (k) for H_2 and D_2 uptake in MFU-4 with exponential fit functions. b) D_2/H_2 selectivity as a function of temperature.

Above this temperature, H_2 diffuses faster than D_2 due to its lower molecular weight. As the temperature decreases, quantum effects appear with D_2 becoming increasingly smaller than H_2 (Figure 2 b and Figure S3, Supporting Information), making D_2 diffuse faster than H_2. Such an effect has only been reported once so far for carbon molecular sieve Takeda 3A, for which quasielastic neutron scattering studies have shown that D_2 diffuses faster below 100 K and slower above this temperature.[20] The D_2/H_2 adsorption selectivity is determined as the ratio of k values for D_2 and H_2 ($S_{D2/H2} = k_{D2}/k_{H2}$) depending on the temperature (Figure 1 b).

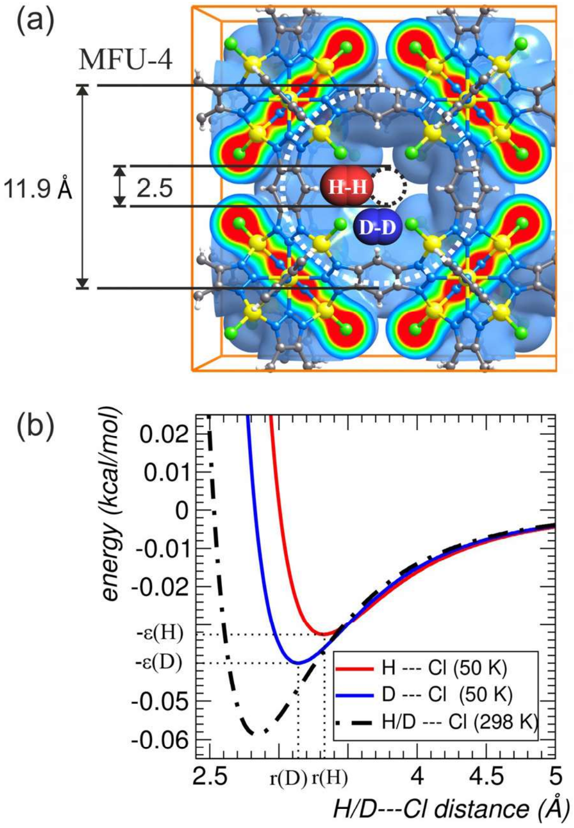

Figure 2. a) Narrow pore aperture (black dashed circle) and large cavity (white dashed circle) in the MFU-4 framework. b) H/D–Cl interactions using the quantum approach at 50 K and the classic limit (298 K).

MFU-4 is selective to deuterium for temperatures lower than T_c and reaches the maximum selectivity $S_{D2/H2}$ of 1.35 at the lowest temperature investigated of 27.5 K (slightly beyond the carrier gas boiling point). By exponentially extrapolating the function for lower temperatures, the maximum selectivity $S_{D2/H2}$ is expected with a factor of 1.45 at 23.6 K (just before D_2 condenses at 23.57 K).

In contrast to previous investigations,[21] in the current study, the exposure of the framework to gas pulses containing H_2 (D_2) occurs in a very short period of less than 30 s and the gases were introduced in the presence of a carrier gas (neon). Comparing these different conditions, we think that in the present investigations the total loading of MFU-4 with hydrogen gas is much lower than in the previous studies, ruling out a direct comparison of the selectivity values. Selectivities are expected to be dependent on the concentration of hydrogen molecules within the pores.

It is very likely that nonadiabatic phononic modes can be stimulated by SAWs, which differ from those at thermal equilibrium. Hence, we cannot rule out the possibility that the gas uptake and release rates measured for MOF@SAW sensors differ strongly from values obtained by other methods. However, we do not claim that our current approach is suitable for yielding diffusion values which can easily be quantified based on first principles. Yet our approach is capable of demonstrating kinetic quantum sieving effects at real time, which, to the best of our knowledge, has not been demonstrated previously.

To rationalize our experimental findings, we have performed a molecular dynamics (MD) study on H_2/D_2 QS in MFU-4. Previous studies suggest that computational modelling provides good support for the interpretation of QS experiments on MOFs[5,10,22] and carbon nanotubes.[8,23,24] MD has scarcely been employed in previous work, such as on zeolite Rho,[25] microporous aluminophosphate $AlPO_4$,[26] and on carbon nanotubes.[13] This is the first MD simulation regarding QS of H_2 and D_2 on MOFs using a flexible framework approach.

A crucial point to which we have paid particular attention is the use of an accurate force field to describe the interactions of the hydrogen molecule with the atoms of the microporous material. The general strategy is to add the quantum Feynmann–Hibbs (FH) correction to the classic Lennard–Jones 12-6 potential. Previous works employ the FH correction up to the quadratic[8,10,27] or the quartic[5,25,28,29] terms. However, the quadratic approximation neglects 20 % of the total quantum correction at 65 K, and this increases to above 50 % for temperatures of 50 K and lower.[25] Hence, we have included up to the 4th order term in the FH correction.

On the other hand, although charge(MOF)–quadrupole(H_2) interactions are important in MOFs with open metal sites,[30] they are less important when no open metal sites exist, as in MFU-4, and here we have neglected this electrostatic effect.

For the MD runs we employed the NVT ensemble using a fully flexible model of MFU-4 using a cubic cell of 21.6 Å. Six different loadings were considered using both pure (H_2 or D_2) and mixed (H_2/D_2) components. Each run was simulated for 10 ns and carried out 5 times with different initial conditions to give statistically accurate data. The MD results show that, for all temperatures in the range of 30–90 K, both H_2 and D_2 are able to diffuse through MFU-4, eventually crossing the small pore gate and filling the next large cavity in an activated motion (Figure 3).

The diffusion coefficients obtained (Table 1) indicate the preferential diffusion of H_2 at the higher temperatures ($>$50–60 K) and of D_2 at the lower temperatures ($<$50–60 K). Agreement with experiments on the selectivities is good, except at the lowest temperature (30 K) at which quantum effects dominate.

In summary, we have successfully applied a recently developed and optimized MOF@SAW sensor setup for precise dynamic measurements on H_2/D_2 quantum sieving in the metal organic framework MFU-4 in the wide temperature range of 27.5–207.1 K. The current studies clearly reveal a quantum sieving phenomenon, in which MFU-4, being selective to H_2 above 64 K, reverses its behaviour and shows faster uptake of D_2 below this temperature. The experimental results obtained are confirmed by MD simulations, also showing that diffusion coefficients for D_2 are higher below (and lower above) 60 K, as compared to H_2. These findings give new insights into kinetic QS in very narrow pores and underline the great potential of MOF@SAW sensors for studying and optimizing gas separation processes including those based on quantum effects and taking place at very low temperatures.

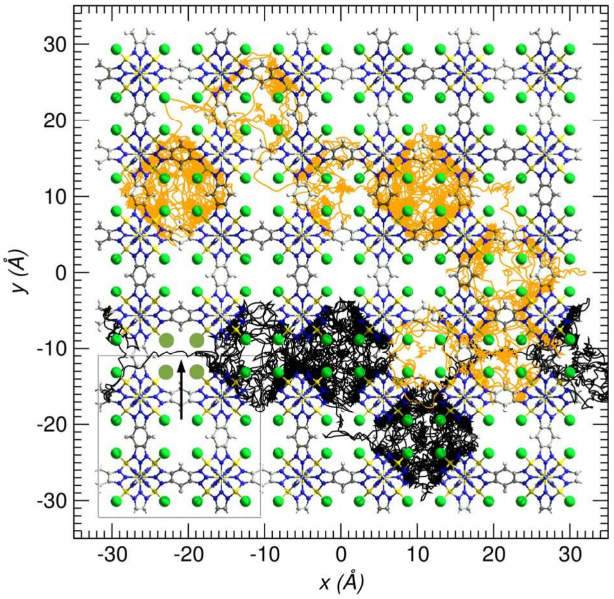

Figure 3. Selected trajectories of two D_2 molecules (black and orange) in MFU-4 at 50 K showing a long residence time in the large pore, but also with some narrow pore crossing. A narrow pore crossing event is indicated by an arrow, with the Cl ligands defining the pore highlighted.

Table 1. Diffusion coefficients $(10\text{–}1^{8}\ \mathrm{cm^2\,s^{-1}})$ of H_2 and D_2 in MFU-4 obtained from molecular dynamics (at a loading of 20 molecules per unit cell) in pure component (p) and 1:1 mixture (m) in the 30–90 K interval. The right column shows the experimentally determined D_2/H_2 selectivities.

T [K]	H_2 (p)	D_2 (p)	D_2/H_2 (p)	D_2/H_2 (exp)
90	4822.9	4032.9	0.84	0.93
80	4386.8	3556.5	0.81	0.95
60	2277.0	2034.8	0.89	1.02
50	1039.5	1302.1	1.25	1.08
40	409.6	560.8	1.37	1.16
30	54.7	136.7	2.50	1.30

T [K]	H_2 (m)	D_2 (m)	D_2/H_2 (m)
90	4950.2	2452.0	0.50
30	45.4	150.5	3.31

Experimental Section

Experimental setup of the SAW sensor

For the experimental observation of the gas adsorption characteristic in porous materials, the frequency generator stimulates the SAWs on the chip at a resonance frequency f_{SAW} of 166 MHz with a power level P_{SAW} of 10 dBm. This is a pulsed signal with a pulse width P_w of 150 ns and a pulse period Pa of 60 μs. The SAW chip itself consists of three Interdigital Transducers (IDTs), each with a finger period λ_{SAW} of 70 μm (Split2), two delay lines for signal and reference measurements with SAW propagation paths d_{SAW} 2 mm, as well as a thermal conductivity detector for monitoring the gas flow.

The sensitivity and temporal response of this thermal conductivity detector has been investigated using a chopped light source and then comparing the sensor response to a fast light detector diode $\tau \approx 20$ ns). It turns out that, depending on the specific gas pulses due to their different heat conductivity, the lower limit for the temporal resolution is $\tau \approx 0{,}3$ ms at a chop frequency of $f = 1$ kHz. For slower pulse trains, as being used in the present experiments, the cooling power of the passing gases can be safely assumed to directly follow the test gas concentration in the carrier gas. For a pure H_2 pulse in N_2, for example, the "contrast" between the heat conductivities of both gases is about seven.

The active area of the sensor ($S_a = 1 \times 1.5$ mm) is covered with a monolayer of MFU-4-coated single crystals with an edge $a_{\text{MFU-4}}$ up to 200 nm. The two SAW signals are first amplified by a preamplifier and subsequently processed analogously and digitally. For noise suppression during measurement, the integral is formed over 30 measured samples and filtered by arguments of 100 μs. All devices are computer controlled and synchronized with the measured data using LabView software in the computer. The mass flow parameters for the test and carrier gas are set to a rate r_{flow} of 100 mL min^{-1}, corresponding to a flow velocity v_{flow} of 0.53 m s^{-1} in the gas pipe line with a laminar flow. The temperature settings at the respective measuring points are controlled by the adjustable gaseous/liquid helium flow and a heating coil in the cryostat.

In previous investigations in our group,[21] MFU-4 samples were loaded with H_2/D_2 gas mixtures at different temperatures (sample exposure times ranged from minutes to hours. The H_2/D_2 loaded samples were subsequently investigated by temperature programmed desorption, from which the total amounts of the adsorbed gas was quantified.

In contrast, in the current study the exposure of the framework to gas pulses containing H_2 (D_2) occurs in a period of less than 30 s and the gases were introduced in the presence of a carrier gas (neon). During the experiments, pure (100 %) H_2 and D_2 pulses, respectively, were added to the carrier gas, simultaneously switching off the carrier gas flow. Thus, disregarding any possible interdiffusing and hence not very well defined but short gas pulse interfaces, a train of carrier gas and pure H_2/D_2 pulses was created which reached the sample after thermalization. Comparing these different conditions, in this study the total loading of MFU-4 with hydrogen gas is much lower than in the previous study, ruling out a direct comparison of the selectivity values. Selectivities are expected to be dependent on the concentration of hydrogen molecules within the pores.

Moreover, in the present investigation a monolayer of nano-sized MFU-4 crystals was deposited on a piezoelectric substrate and during gas exposure time, (low power) surface acoustic waves were applied, possibly accounting for elastic deformation at normal direction to the surface in the order of one nanometer or less and typical field strength of 1–5 kV cm^{-1}. The exact impact of the distortion of flexible MOFs in the presence of strong electric fields is not taken into account by the molecular dynamics calculations, nor have we experimentally investigated this effect by varying the SAW power, so far. Electric fields can exert a strong influence on the mechanical properties of soft materials such as metal–organic frameworks, as can be seen in a previous publication.[31]

MFU-4 is a cubic framework possessing relatively large cavities, 11.9 Å in diameter, interconnected by very narrow apertures of 2.5 Å (the distance between chloride ligands, cf. Figure 2). This construction, with a large and expanding variety of metals and linkers,[32] allows for size-dependent sieving of adsorbate molecules and offers a large pore volume for the uptake of adsorbed species. MFU-4 was shown to perform H_2/D_2 QS with a maximum selectivity of 7.5, as determined by thermal desorption spectroscopy after loading the sample with a 1:1 H_2/D_2 mixture at 60 K,[21] although on a different experimental setup (Section S1, Supporting Information). Previous studies on several Zeolitic Imidazolate Frameworks

(ZIFs) and COFs have shown that the maximum D_2/H_2 selectivity is achieved with the ZIF-8 framework having pores of 3.4 Å diameter, whereas the ZIF-7 framework with 3.0 Å pores does not show any H_2 or D_2 uptake at all.[11] In contrast, MFU-4, possessing even smaller pore apertures of 2.5 Å, still shows uptake of both gases due to the flexibility of its narrow pores, which arises from the floppiness of the Cl-Zn-N angles, with a very small value of the bending constant (18.5 kcal mol^{-1}) as indicated in Table S2, Supporting Information.[33]

Acknowledgements

D.V. and A.W. are grateful for financial support by DFG: priority program 1928 "Coordination Networks: Building Blocks for Functional Systems". This work was supported in part by the Cluster of Excellence NIM (Nanosystems Initiative Munich) of the German Government. B.P. gratefully acknowledges financial support by the Bavarian Science Foundation. G.S. thanks MINECO of Spain for funding (SEV-2016-0683 and MAT2015-71842-P) and ASIC-UPV for the use of computational facilities.

Conflict of interest

The authors declare no conflict of interest.

Keywords: diffusion kinetic · isotope separation · metal-organic frameworks · quantum sieving · surface acoustic waves

[1] H. Oh, M. Hirscher, *Eur. J. Inorg. Chem.* **2016**, 4278–4289.

[2] J. J. M. Beenakker, V. D. Borman, S. Yu. Krylov, *Chem. Phys. Lett.* **1995**, *232*, 379–382.

[3] a) X. Zhao, S. Villar-Rodil, A. J. Fletcher, K. M. Thomas, *J. Phys. Chem. B* **2006**, *110*, 9947–9955; b) I. Krkljus, T. Steriotis, G. Charalambopoulou, A. Gotzias, M. Hirscher, *Carbon* **2013**, *57*, 239–247; c) Y. Xing, J. Cai, L. Li, M. Yang, X. Zhao, *Phys. Chem. Chem. Phys.* **2014**, *16*, 15800–15805.

[4] G. Garberoglio, *Chem. Phys. Lett.* **2009**, *467*, 270–275.

[5] D. Liu, W. Wang, J. Mi, C. Zhong, Q. Yang, D. Wu, *Ind. Eng. Chem. Res.* **2012**, *51*, 434–442.

[6] J. Cai, Y. Xing, X. Zhao, *RSC Adv.* **2012**, *2*, 8579–8586.

[7] F. Stéphanie-Victoire, A. Goulay, E. Cohen de Lara, *Langmuir* **1998**, *14*, 7255–7259.

[8] H. Tanaka, H. Kanoh, M. Yudasaka, S. Iijima, K. Kaneko, *J. Am. Chem. Soc.* **2005**, *127*, 7511–7516.

[9] B. Chen, X. Zhao, A. Putkham, K. Hong, E. B. Lobkovsky, E. J. Hurtado, A. Fletcher, K. M. Thomas, *J. Am. Chem. Soc.* **2008**, *130*, 6411–6423.

[10] D. Noguchi, H. Tanaka, A. Kondo, H. Kajiro, H. Noguchi, T. Ohba, H. Kanoh, K. Kaneko, *J. Am. Chem. Soc.* **2008**, *130*, 6367–6372.

[11] H. Oh, K. S. Park, S. B. Kalidindi, R. A. Fischer, M. Hirscher, *J. Mater. Chem. A* **2013**, *1*, 3244–3248.

[12] H. Oh, S. B. Kalidindi, Y. Um, S. Bureekaew, R. Schmid, R. A. Fischer, M. Hirscher, *Angew. Chem. Int. Ed.* **2013**, *52*, 13219–13222; *Angew. Chem.* **2013**, *125*, 13461–13464.

[13] S. Niimura, T. Fujimori, D. Minami, Y. Hattori, L. Abrams, D. Corbin, K. Hata, K. Kaneko, *J. Am. Chem. Soc.* **2012**, *134*, 18483–18486.

[14] S. Biswas, M. Grzywa, H. P. Nayek, S. Dehnen, I. Senkovska, S. Kaskel, D. Volkmer, *Dalton Trans.* **2009**, *33*, 6487–6495.

[15] a) H. Wohltjen, R. Dessy, *Anal. Chem.* **1979**, *51*, 1458–1464; b) P. Hess, *Phys. Today* **2002**, *55*, 42–47; c) J. W. Grate, *Chem. Rev.* **2000**, *100*, 2627–2648; d) F. A. Bahos, A. Sainz-Vidal, C. Sánchez-Perez, J. M. Saniger, I. Gràcia, M. M. Saniger-Alba, D. Matatagui, *Biosensors* **2019**, *9*, 4; e) J. Devkota, K.-J. Kim, P. R. Ohodnicki, J. T. Culp, D.-W. Greve, J. W. Lekse, *Nanoscale* **2018**, *10*, 8075–8087.

[16] B. Paschke, A. Wixforth, D. Denysenko, D. Volkmer, *ACS Sens.* **2017**, *2*, 740–747.

[17] L. E. Kreno, K. Leong, O. K. Farha, M. Allendorf, R. P. Van Duyne, J. T. Hupp, *Chem. Rev.* **2012**, *112*, 1105–1125.

[18] I. Stassen, N. Burtch, A. Talin, P. Falcaro, M. Allendorf, R. Ameloot, *Chem. Soc. Rev.* **2017**, *46*, 3185–3241.

[19] R. M. White, F. W. Voltmer, *Appl. Phys. Lett.* **1965**, *7*, 314–316.

[20] T. X. Nguyen, H. Jobic, S. K. Bhatia, *Phys. Rev. Lett.* **2010**, *105*, 085901.

[21] J. Teufel, H. Oh, M. Hirscher, M. Wahiduzzaman, L. Zhechkov, A. Kuc, T. Heine, D. Denysenko, D. Volkmer, *Adv. Mater.* **2013**, *25*, 635–639.

[22] H. Oh, I. Savchenko, A. Mavrandonakis, T. Heine, M. Hirscher, *ACS Nano* **2014**, *8*, 761–770.

[23] Q. Wang, S. R. Challa, D. Sholl, J. K. Johnson, *Phys. Rev. Lett.* **1999**, *82*, 956–959.

[24] S. R. Challa, D. S. Sholl, J. K. Johnson, *J. Chem. Phys.* **2002**, *116*, 814–824.

[25] A. V. A. Kumar, S. K. Bhatia, *Phys. Rev. Lett.* **2005**, *95*, 245901.

[26] A. V. A. Kumar, S. K. Bhatia, *J. Phys. Chem. C* **2008**, *112*, 11421–11426.

[27] Y. Peng, G. Srinivas, C. E. Wilmer, I. Eryazici, R. Q. Snurr, J. T. Hupp, T. Yildirim, O. K. Farha, *Chem. Commun.* **2013**, *49*, 2992–2994.

[28] J. L. Belof, A. C. Stern, B. Space, *J. Chem. Theory Comput.* **2008**, *4*, 1332–13337.

[29] J. Fu, H. Sun, *J. Phys. Chem. C* **2009**, *113*, 21815–21824.

[30] J. Liu, R. B. Rankin, J. K. Johnson, *Mol. Simul.* **2009**, *35*, 60–69.

[31] A. Knebel, B. Geppert, K. Volgmann, D. I. Kolokolov, A. G. Stepanov, J. Twiefel, P. Heitjans, D. Volkmer, J. Caro, *Science* **2017**, *358*, 347–351.

[32] I. Weinrauch, I. Savchenko, D. Denysenko, S. M. Souliou, H.-H. Kim, M. Le Tacon, L. L. Daemen, Y. Cheng, A. Mavrandonakis, A. J. Ramirez-Cuesta, D. Volkmer, G. Schütz, M. Hirscher, T. Heine, *Nat. Commun.* **2017**, *8*, 14496.

[33] G. Sastre, J. Van Den Bergh, F. Kapteijn, D. Denysenko, D. Volkmer, *Dalton Trans.* **2014**, *43*, 9612–9619.